Supporting Information

Exploitation of Conformational Dynamics in Imparting Selective Inhibition for Related Matrix Metalloproteinases

Kiran V. Mahasenan,[†] Maria Bastian,[†] Ming Gao,[†] Emma Frost,[†] Derong Ding,[†] Katerina Zorina-Lichtenwalter,[†] John Jacobs,[†] Mark A. Suckow,[‡] Valerie A. Schroeder,[‡] William R. Wolter,[‡] Mayland Chang[†*] and Shahriar Mobashery[†*]

*S.M.: E-mail, mobashery@nd.edu; Phone, +1-574-631-2933
*M.C.: E-mail, mchang@nd.edu, Phone, +1-574-631-2965

[†]Department of Chemistry and Biochemistry, University of Notre Dame, Notre Dame, Indiana 46556, USA.

[‡]Freimann Life Science Center and Department of Biological Sciences, University of Notre Dame, Notre Dame, Indiana 46556, USA.

Table of contents

Figure S1. Ω-Loop sequence alignment for the 23 members of human MMPs.

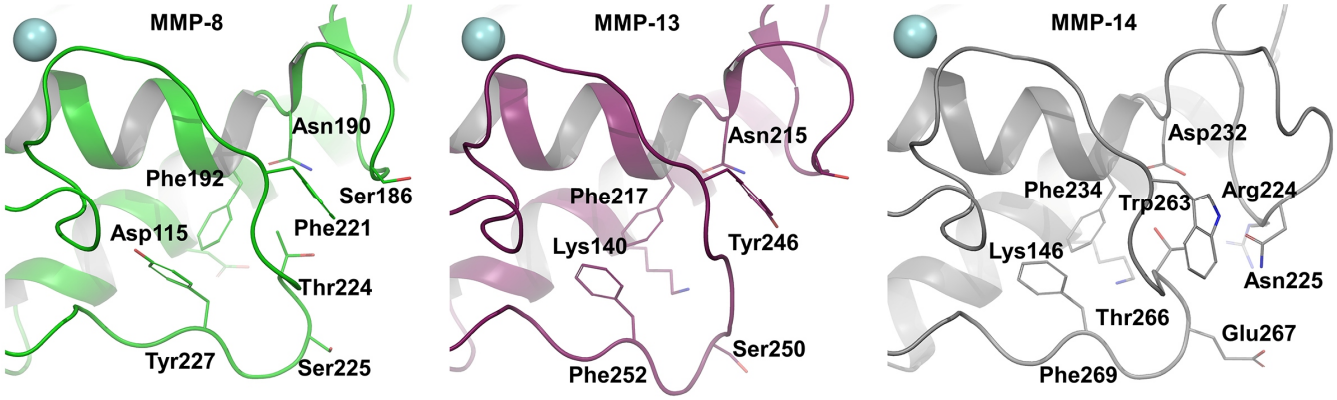

Figure S2. Comparison of the inhibitor **1** binding-site in the X-ray structures of MMP-8, MMP-13, and MMP-14 S1′ pocket, showing a selected set of relevant residues.

Table S1. Residues in the MMP S1′ pocket within 5 Å of benzoxazinone template. Key residues are highlighted in bold letters.

#	MMP-8	MMP-13	MMP-14
1	LEU119	VAL144	VAL150
2	PHE192	PHE217	PHE234
3	LEU193	LEU218	LEU235
4	GLY212	GLY237	SER254
5	ALA213	ALA238	ALA255
6	LEU214	LEU239	ILE256
7	ALA220	THR245	GLN262
8	PHE221	TYR246	TRP263
9	ARG222	THR247	MET264
10	**GLU223**	**GLY248**	**ASP265**
11	THR224	LYS249	THR266
12	**SER225**	**SER250**	**GLU267**
13	ASN226	HIS251	ASN268
14	**TYR227**	**PHE252**	**PHE269**
15	SER228	MET253	VAL270
16	LEU229	LEU254	LEU271
17	PRO230	PRO255	PRO272

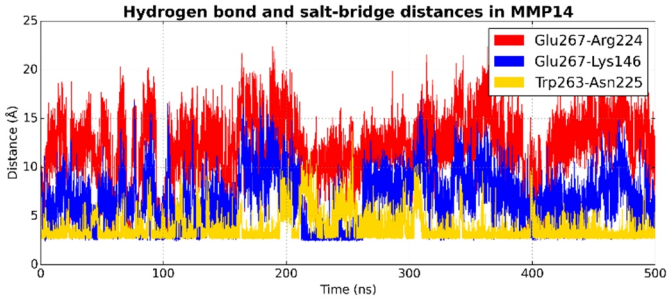

Figure S3. Interaction of MMP14 S1′ loop residues with the neighboring residues render the S1′ pocket rigid.

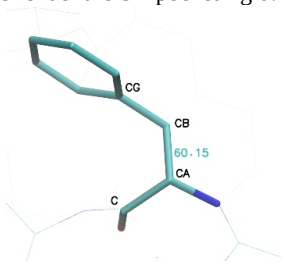

Figure S4. Dihedral angle of atoms C-Cα-Cβ-CG defines side-chain rotamers based on the Cα-Cβ bond torsional axis.

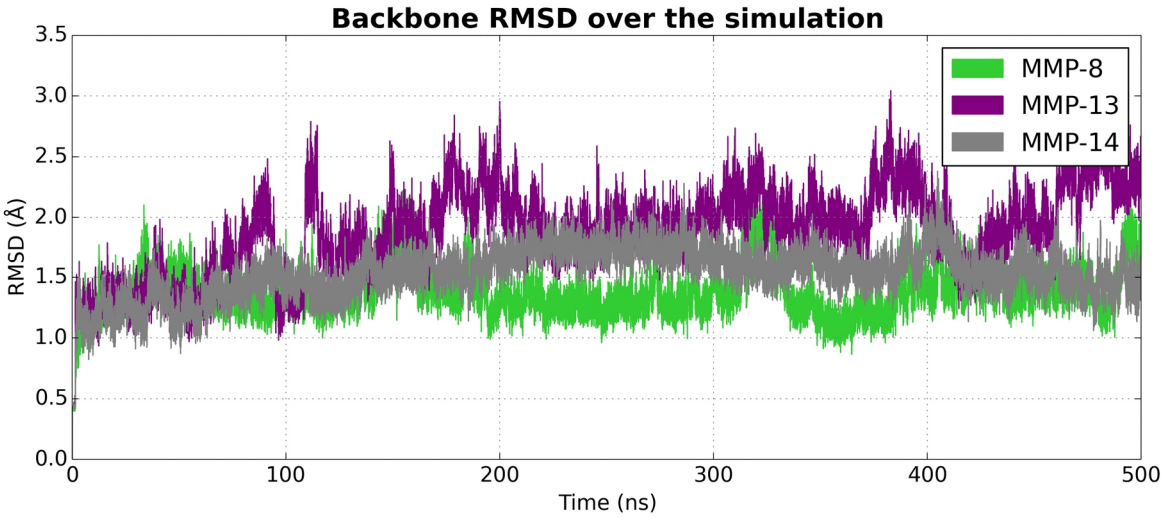

Figure S5. Flexibility of MMPs during 500 ns MD simulation as demonstrated by the backbone (C, CA, and N atoms) RMSD of the catalytic domain.

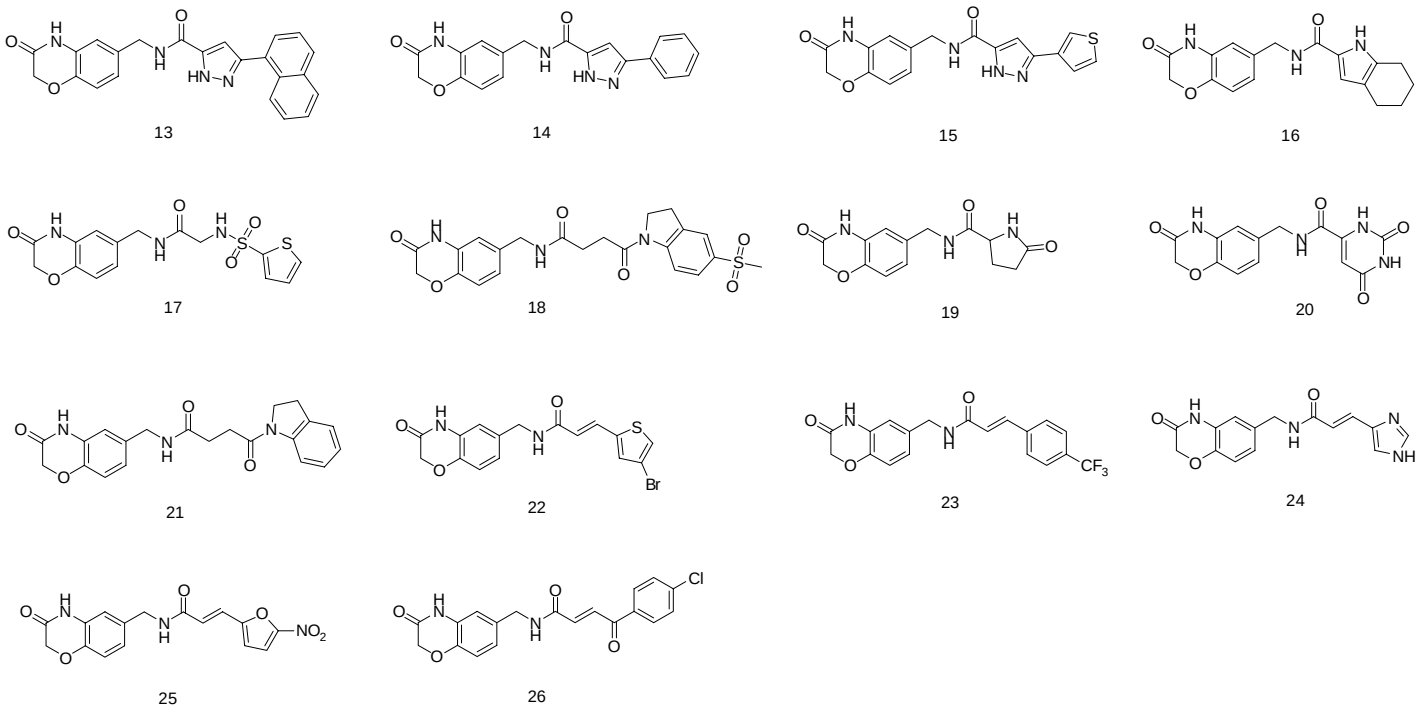

Figure S6. The benzoxazinone analogs that were prepared, which exhibited relatively poor inhibition or no inhibition of MMPs.

Table S2. Kinetic parameters for inhibition of MMPs

Compounds	K_i (nM)							
	MMP-1	**MMP-2**	**MMP-3**	**MMP-7**	**MMP-8**	**MMP-9**	**MMP-13**	**MMP-14**
1[1]	24000 ± 3000	3000 ± 200	17000 ± 2000	53000 ± 6000	25 ± 2	76000 ± 8000	0.53 ± 0.30	45000 ± 4000
8	8%[a]	18%[a]	NI[b]	11%[a]	8500 ± 1400[c]	7%[a]	36 ± 11[c]	1%[a]
9	NI[b]	3%[a]	23%[a]	2%[a]	6500 ± 900[c]	NI[b]	190 ± 14[c]	4%[a]
10	28%[d]	1500 ± 100[c]	67%[a]	8%[d]	19 ± 5[e]	26%[a]	0.47 ± 0.06[e]	14%[a]
11	13%[a]	54%[a]	26%[a]	11%[a]	3.3 ± 0.17[c]	37%[a]	24.5 ± 3[c]	57%[d]
12	38%[d]	6400 ± 970[f]	58%[d]	18%[d]	0.71 ± 0.04[e]	8800 ± 250[f]	0.59 ± 0.07[e]	14%[a]
13	NI[b]	35%[a]	8500 ± 700[c]	3%[a]	2200 ± 300[c]	7%[a]	4100 ± 700[g]	NI[b]
14	NI[b]	25000 ± 2000[c]	16%[a]	16%[a]	35%[a]	11%[a]	1000 ± 100[g]	NI[b]
15	2%[a]	9800 ± 500[c]	8%[a]	5%[a]	38%[a]	NI[b]	4400 ± 700[c]	1%[a]
16	12%[a]	22%[a]	9%[a]	36%[a]	NI[b]	NI[b]	28%[a]	NI[b]
17	10%[a]	20%[a]	10%[a]	NI[b]	25%[a]	NI[b]	27%[a]	NI[b]
18	2%[a]	NI[b]	NI[b]	1%[a]	NI[b]	25%[a]	3%[a]	6%[a]
19	20%[a]	19%[a]	18%[a]	11%[a]	20%[a]	39%[a]	9%[a]	5%[a]
20	10%[a]	8%[a]	NI[b]	NI[b]	21%[a]	8%[a]	3%[a]	3%[a]
21	10%[a]	19%[a]	NI[b]	9%[a]	NI[b]	14%[a]	12%[a]	NI[b]
22	NI[b]	18%[a]	NI[b]	17%[a]	NI[b]	NI[b]	13%[a]	7%[a]
23	4%[a]	5%[a]	2%[a]	NI[b]	NI[b]	NI[b]	NI[b]	NI[b]
24	4%[a]	9%[a]	3%[a]	1%[a]	NI[b]	NI[b]	NI[b]	NI[b]
25	NI[b]	8%[a]	10%[a]	8%[a]	2%[a]	2%[a]	35%[a]	7%[a]
26	NI[b]	NI[b]	7%[a]	6%[a]	2%[a]	NI[b]	NI[b]	NI[b]

[a]Inhibition at 10 μM. [b]No inhibition at 10 μM. [c]Linear-competitive inhibition. [d]Inhibition at 50 μM. [e]Tight-binding. [f]Linear-uncompetitive inhibition. [g]Linear-noncompetitive inhibition.

Syntheses. The synthesis of compound 8 given in Scheme 1 is provided here as a representative method for preparation of these compounds. The same reaction conditions were applied to obtain the other compounds listed in Table 1. Purity of all final products was determined to be ≥ 95%, as confirmed by UPLC and NMR. Detailed conditions are provided in the UPLC section.

Ethyl-2-cyano-3-(4-(trifluoromethyl)phenyl)but-2-enoate (3). A solution of 4-acetylbenzotrifluoride **2** (1 g, 5.3 mmol) and ethyl cyanoacetate (780 mg, 6.9 mmol) in 18 mL toluene was placed in a round-bottom flask and was set up with a Dean-Stark apparatus. Acetic acid (0.3 mL, 5.3 mmol) and piperidine (0.52 mL, 5.3 mmol) were added before the mixture was refluxed for 20 hours. The resulting solution was cooled to room temperature and toluene was removed *in vacuo*. Purification by column chromatography on silica gel (EtOAc/hexane, 1:4) yielded the product as a nearly equal mixture of both geometric isomers (yellow oil, 840 mg, 56%). Major isomer: ^{1}H NMR (600 MHz, $CDCl_3$) δ 1.39 (t, *J* = 7.1 Hz, 3H), 2.70 (s, 3H), 4.36 (q, *J* = 7.1 Hz, 2H), 7.54 (d, *J* = 8.1 Hz, 2H), 7.72 (d, *J* = 8.2 Hz, 2H); ^{13}C NMR (100 MHz, $CDCl_3$) δ 14.1, 23.2, 62.4, 106.7, 115.6, 123.7 (q, *J* = 270,7 Hz), 125.9 (q, *J* = 3.8 Hz, 2C), 127.6 (2C), 132.0 (q, *J* = 32.7 Hz), 143.8, 161.9, 170.4; Minor isomer: 1H NMR (600 MHz, $CDCl_3$) δ 1.15 (t, *J* = 7.1 Hz, 3H), 2.55 (s, 3H), 4.11 (q, *J* = 7.1 Hz, 2H), 7.28 (d, *J* = 8.0 Hz, 2H), 7.67 (d, *J* = 8.1 Hz, 2H); ^{13}C NMR (100 MHz, $CDCl_3$) δ 13.7, 27.1, 62.3, 107.5, 115.1, 123.9 (q, *J* = 270,7 Hz), 125.5 (q, *J* = 3.8 Hz, 2C), 126.6 (2C), 131.1 (q, *J* = 32.7 Hz), 142.8, 160.9, 168.3; HRMS (ESI): calcd for $C_{14}H_{12}F_3NNaO_2$ $[M+Na]^+$ 306.0712, found 306.0706.

Ethyl 2-amino-4-(4-(trifluoromethyl)phenyl)thiophene-3-carboxylate (4). Sulfur (231 mg, 7.2 mmol) was added to a solution of compounds **3** (2 g, 7.1 mmol) in 40 mL methanol. The resulting suspension was heated to 50 °C and diethylamine (0.37 mL, 3.6 mmol) was added dropwise. After stirring the mixture for 4 hours at 50 °C, the solvent was removed *in vacuo* and the crude product was purified by column chromatography on silica gel (EtOAc/hexane, 1:4) yielding the product as a white solid (1.88 g, 84%). ^{1}H NMR (400 MHz, $CDCl_3$) δ 0.92 (t, *J* = 7.1 Hz, 3H), 4.04 (q, *J* = 7.1 Hz, 2H), 6.09 (s, 1H), 6.13 (s, 2H), 7.41 (d, *J* = 7.92 Hz, 2H), 7.58 (d, *J* = 8.6 Hz, 2H); ^{13}C NMR (100 MHz, $CDCl_3$) δ 13.8, 59.7, 106.4, 124.3 (q, *J* = 3.8 Hz, 2C), 124.4 (q, *J* = 270.2 Hz), 129.3 (q, *J* = 32.1 Hz), 129.3, 129.5 (2C), 140.4, 142.4, 164.2, 165.5; HRMS (ESI): calcd for $C_{14}H_{13}F_3NO_2S$ $[M+H]^+$ 316.0614, found 316.0620.

Ethyl 4-oxo-5-(4-(trifluoromethyl)phenyl)-3,4-dihydrothieno[2,3-d]pyrimidine-2-carboxylate (5). Compound **4** (640 mg, 2 mmol) was dissolved in 1.3 mL of 4M HCl in dioxane and ethyl cyanoformate (0.33 mL, 3.3 mmol) was added. The resulting mixture was stirred for 2 hours at 50 °C before the solvent was removed *in vacuo.* The crude product was dissolved in EtOAc and was washed with brine, dried over Na_2SO_4 and concentrated *in vacuo*. Purification by column chromatography on silica gel (MeOH/DCM, 1:19) yielding the product as a yellow solid (204 mg, 28%). ^{1}H NMR (400 MHz, DMSO-d_6) δ 1.36 (t, *J* = 7.1 Hz, 3H), 4.39 (q, *J* = 7.1 Hz, 2H), 7.76 (m, 4H), 7.89 (s, 1H), 12.90 (s, 1H); ^{13}C NMR (100 MHz, DMSO) δ 13.8, 62.8, 122.4, 124.4 (q, *J* = 3.8 Hz, 2C), 124.5 (q, *J* = 270.4 Hz), 125.8, 127.8 (q, *J* = 31.6 Hz), 130.1 (2C), 137.0, 138.8, 143.8, 157.2, 159.5, 164.0; HRMS (ESI): calcd for $C_{16}H_{12}F_3N_2O_3S$ $[M+H]^+$ 369.0515, found 369.0528.

4-Oxo-5-(4-(trifluoromethyl)phenyl)-3,4-dihydrothieno[2,3-d]pyrimidine-2-carboxylic acid (6). To a solution of ester **4** (2 g, 5.4 mmol) in 80 mL THF was added a 1 M solution of LiOH in water (8 mL). After stirring for 1 hour at room temperature, the pH was adjusted to 1.0 using aqueous 1 M HCl. The precipitate was filtered and the filtrate was washed with hexane to give the product as white solid (1.64 g, 98%). ^{1}H NMR (600 MHz, DMSO-d_6) δ 7.77 (m, 4H), 7.88 (s, 1H), 12.70 (s, 1H); ^{13}C NMR (150 MHz, DMSO) δ 122.3, 124.5 (q, *J* = 270.5 Hz), 124.5 (q, *J* = 3.8 Hz, 2C), 125.7, 128.0 (q, *J* = 31.4 Hz), 130.3 (2C), 137.1, 139.0, 144.9, 157.4, 161.1, 164.3; HRMS (ESI): calcd for $C_{14}H_8F_3N_2O_3S$ $[M+H]^+$ 341.0202, found 341.0201.

4-Oxo-N-((3-oxo-3,4-dihydro-2H-benzo[1,4]oxazin-6-yl)methyl)-5-(4-(trifluoromethyl)phenyl)-3,4-dihydrothieno[2,3-d]pyrimidine-2-carboxamide (8). 1-[Bis(dimethylamino)methylene]-1H-1,2,3-triazolo[4,5-b]pyridinium 3-oxide hexafluorophosphate (HATU) (260 mg, 0.7 mmol) and 4-Methylmorpholine (NMM) (0.14 mL, 1.3 mmol) were added to an solution of acid **6** (200 mg, 0.5 mmol) in 6 mL DMF. The reaction was stirred for 30 minutes at room temperature before 6-(aminomethyl)-2H-benzo[1,4]oxazin-3(4H)-one hydrochloride **7** (132 mg, 0.6 mmol) was added and stirred overnight. The solvent was partially removed *in vacuo* and water was added to the remaining oil, forming a white precipitate. Filtration and washing with hexane yielded the desired crude product. The solid was dissolved in minimal DMSO and water was added dropwise under vigorous stirring, until no additional precipitate formed. The solid was filtered and washed with hexane, yielding the desired product **8** with a purity of more than 95% as a white solid (190 mg, 71%). ^{1}H NMR (600 MHz, DMSO-d_6) δ 4.36 (d, *J* = 6.3, 2H), 4.53 (s, 2H), 6.89 (m, 1H), 6.91 (m, 2H), 7.76 (m, 4H), 7.84 (s, 1H), 9.71 (t, *J* = 6.6, 1H), 10.70 (s, 1H), 12.38 (s, 1H); ^{13}C NMR (100 MHz, DMSO) δ 42.3, 66.7, 115.1, 115.9, 121.9, 122.4, 124.3 (q, *J* = 270.4 Hz), 124.4 (q, *J* = 3.7 Hz, 2C), 124.7, 127.1, 127.8 (q, *J* = 31.5 Hz), 130.1 (2C), 132.9, 137.0, 138.9, 142.3, 146.3, 157.1, 158.7, 163.8, 164.9; HRMS (ESI): calcd for $C_{23}H_{16}F_3N_4O_4S$ $[M+H]^+$ 501.0839, found 501.0859.

4-Oxo-N-((3-oxo-3,4-dihydro-2H-benzo[1,4]oxazin-6-yl)methyl)-5-phenethyl-3,4-dihydrothieno[2,3-*d*]pyrimidine-2-carboxamide (9). Compound **9** was synthesized following the synthetic pathway described for compound **8** in Scheme 1 of the main text (51 mg, 81%). ^{1}H NMR (600 MHz, DMSO-d_6) δ 2.29 (m, 2H), 3.18 (m, 2H), 4.34 (d, *J* = 6.4, 2H), 4.52 (s, 2H), 6.88 (m, 1H), 6.90 (m, 2H), 7.18 (m, 1H), 7.25 (m, 2H), 7.28 (m, 2H), 7.33 (s, 1H), 9.63 (t, *J* = 6.4, 1H), 10.68 (s, 1H), 12.31 (s, 1H); ^{13}C NMR (100 MHz, DMSO) δ 31.8, 35.7, 42.2, 66.7, 115.0, 115.8, 120.7, 122.3, 123.4, 125.7, 127.0, 128.1 (2C), 128.3 (2C), 132.8, 138.3, 141.4, 142.2, 145.7, 157.6, 158.7, 163.0, 164.8; HRMS (ESI): calcd for $C_{24}H_{21}N_4O_4S$ $[M+H]^+$ 461.1278, found 461.1268.

5-cyclohexyl-4-oxo-N-((3-oxo-3,4-dihydro-2H-benzo[b][1,4]oxazin-6-yl)methyl)-3,4-dihydrothieno[2,3-d]pyrimidine-2-carboxamide (10). Compound **10** was synthesized following the previously described synthetic pathway.[1] ^{1}H NMR (500 MHz, DMSO-d_6) δ 1.17-1.24 (m, 1H), 1.31-1.41 (m, 4H), 1.70-1.79 (m, 3H), 1.95 (d, *J* = 10.5 Hz, 2H), 3.27-3.2 9 (m, 1H), 4.33 (d, *J* = 6.5 Hz, 2H), 4.52 (s, 2H), 6.87-6.89 (m, 3H), 7.34 (s, 1H), 9.63 (t, *J* = 6.0 Hz, 1H), 10.68 (s, 1H), 12.29 (s, 1H). ^{13}C NMR (126 MHz, DMSO-d_6) δ 26.4, 26.9, 33.8, 38.6, 42.9, 67.4, 115.7, 116.6, 119.0, 123.0, 123.7, 127.8, 133.6, 143.0, 145.8, 146.2, 158.1, 159.5, 163.7, 165.6. HRMS (*m/z*): $[M + H]^+$, calcd for $C_{22}H_{23}N_4O_4S$, 439.1435; found, 439.1440.

6-cyclohexyl-4-oxo-N-((3-oxo-3,4-dihydro-2H-benzo[b][1,4]oxazin-6-yl)methyl)-3,4-dihydrothieno[2,3-d]pyrimidine-2-carboxamide(11). Compound **11** was synthesized following the previously described synthetic pathway.[1] ^{1}H NMR (500 MHz, DMSO-d_6) δ 1.19-1.26 (m, 1H), 1.34-1.46 (m, 4H), 1.68 (d, *J* = 12.5 Hz, 1H), 1.78 (d, *J* = 12.0 Hz, 2H), 2.01 (d, *J* = 11.0 Hz, 2H), 2.88 (d, *J* = 7.5 Hz, 1H), 4.33 (d, *J* = 6.5 Hz, 2H), 4.52 (s, 2H), 6.87-6.89 (m, 3H), 7.19 (s, 1H), 9.63 (t, *J* = 6.0 Hz, 1H), 10.68 (s, 1H), 12.37 (s, 1H). ^{13}C NMR (126 MHz, DMSO-d_6) δ 25.9, 26.3, 35.1, 42.9, 67.4, 115.8, 116.6, 117.2, 123.0, 126.6, 127.8, 133.7,

143.0, 146.0, 152.2, 157.6, 159.5, 160.8, 165.6. HRMS (*m/z*): [M + H]$^+$, calcd for $C_{22}H_{23}N_4O_4S$, 439.1435; found, 439.1458.

4-oxo-N-((3-oxo-3,4-dihydro-2H-benzo[b][1,4]oxazin-6-yl)methyl)-3,4,5,6,7,8,9,10-octahydrocycloocta[4,5]thieno[2,3-d]pyrimidine-2-carboxamide(12). Compound **12** was synthesized following the previously described synthetic pathway.[1] ^{1}H NMR (500 MHz, DMSO-d_6) δ 1.21-1.26 (m, 2H), 1.38-1.42 (m, 2H), 1.59-1.62 (m, 4H), 2.89 (t, *J* = 5.8 Hz, 2H), 3.06 (t, *J* = 5.8 Hz, 2H), 4.31 (d, *J* = 6.35 Hz, 2H), 4.51 (s, 2H), 6.85-6.87 (m, 3H), 9.60 (t, *J* = 6.25 Hz, 1H), 10.66 (s, 1H), 12.21 (s, 1H). ^{13}C NMR (126 MHz, DMSO-d_6) δ 25.0, 25.9, 26.1, 27.0, 30.5, 32.2, 42.9, 67.4, 115.7, 116.6, 123.0, 124.5, 127.8, 133.7, 135.0, 138.9, 142.9, 145.5, 158.1, 159.5, 160.6, 165.6. HRMS (*m/z*): [M + H]$^+$, calcd for $C_{22}H_{23}N_4O_4S$, 439.1435; found, 439.1435.

3-(Naphthalen-1-yl)-*N*-((3-oxo-3,4-dihydro-*2H*-benzo[1,4]oxazin-6-yl)methyl)-*1H*-pyrazole-5-carboxamide (13). Compound **13** was synthesized following the synthetic pathway described for compound **8** in Scheme 1 of the main text (43 mg, 90%). ^{1}H NMR (600 MHz, DMSO-d_6) δ 4.37 (d, *J* = 6.3, 2H), 4.50 (s, 2H), 6.91 (m, 3H), 6.94 (s, 1H), 7.60 (m, 4H), 8.04 (m, 3H), 8.80 (t, *J* = 5.9, 1H), 10.68 (s, 1H), 13.66 (s, 1H); ^{13}C NMR (100 MHz, DMSO) δ 41.4, 66.7, 106.1, 114.8, 115.7, 122.0, 124.6, 125.3, 125.4, 126.3, 126.6, 127.0 (2C), 128.4, 129.1, 130.4, 133.3, 134.2, 141.7, 142.0, 147.2, 161.6, 164.8; HRMS (ESI): calcd for $C_{23}H_{19}N_4O_3$ [M+H]$^+$ 399.1452, found 399.1472.

***N*-((3-Oxo-3,4-dihydro-*2H*-benzo[1,4]oxazin-6-yl)methyl)-3-phenyl-*1H*-pyrazole-5-carboxamide (14).** Compound **14** was synthesized following the synthetic pathway described for compound **8** in Scheme 1 of the main text (27 mg, 37%). ^{1}H NMR (600 MHz, DMSO-d_6) δ 4.34 (d, *J* = 6.1, 2H), 4.51 (s, 2H), 6.88 (m, 3H), 7.07 (s, 1H), 7.43 (t, *J* = 7.6, 1H), 7.47 (t, *J* = 6.4, 2H), 7.79 (d, *J* = 7.6, 2H), 8.71 (t, *J* = 5.3, 1H), 10.67 (s, 1H), 13.66 (s, 1H); ^{13}C NMR (150 MHz, DMSO) δ 41.4, 66.8, 102.7, 114.9, 115.8, 122.0, 125.3 (2C), 127.0, 128.5, 129.1 (2C), 133.2, 134.3, 142.1, 143.4, 147.8, 161.6, 165.0; HRMS (ESI): calcd for $C_{19}H_{17}N_4O_3$ [M+H]$^+$ 349.1295, found 349.1312.

***N*-((3-Oxo-3,4-dihydro-*2H*-benzo[1,4]oxazin-6-yl)methyl)-3-(thiophen-3-yl)-*1H*-pyrazole-5-carboxamide (15).** Compound **15** was synthesized following the synthetic pathway described for compound **8** in Scheme 1 of the main text (43 mg, 94%). ^{1}H NMR (600 MHz, DMSO-d_6) δ 4.33 (d, *J* = 6.1, 2H), 4.52 (s, 2H), 6.88 (m, 3H), 6.98 (s, 1H), 7.65 (d, *J* = 4.9, 1H), 7.68 (t, *J* = 3.4, 1H), 7.93 (s, 1H), 8.67 (t, *J* = 6.1, 1H), 10.66 (s, 1H), 13.55 (s, 1H); ^{13}C NMR (150 MHz, DMSO) δ 41.4, 66.8, 102.7, 114.9, 115.8, 121.7, 122.0, 125.7, 127.0, 127.6, 130.1, 134.2, 139.5, 142.1, 147.5, 131.6, 165.0; HRMS (ESI): calcd for $C_{17}H_{15}N_4O_3S$ [M+H]$^+$ 355.0859, found 355.0865.

***N*-((3-Oxo-3,4-dihydro-*2H*-benzo[1,4]oxazin-6-yl)methyl)-4,5,6,7-tetrahydro-*1H*-indole-2-carboxamide (16).** Compound **16** was synthesized following the synthetic pathway described for compound **8** in Scheme 1 of the main text (34 mg, 47%). ^{1}H NMR (600 MHz, DMSO-d_6) δ 1.65 (m, 2H), 1.69 (m, 2H), 2.39 (t, *J* = 6.1, 2H), 2.49 (m, 2H), 4.33 (d, *J* = 6.1, 2H), 4.51 (s, 2H), 6.51 (d, *J* = 2.3, 1H), 6.82 (m, 2H), 6.87 (m, 1H), 8.24 (t, *J* = 6.1, 1H), 10.64 (s, 1H), 10.89 (s, 1H); ^{13}C NMR (150 MHz, DMSO) δ 22.4, 22.5, 22.8, 23.4, 41.2, 66.8, 108.9, 114.5, 115.8, 116.9, 121.7, 123.9, 127.1, 130.7, 134.6, 142.0, 160.8, 165.0; HRMS (ESI): calcd for $C_{18}H_{20}N_3O_3$ [M+H]$^+$ 326.1499, found 326.1498.

***N*-((3-Oxo-3,4-dihydro-*2H*-benzo[1,4]oxazin-6-yl)methyl)-2-(thiophene-2-sulfonamido)acetamide (17).** Compound **17** was synthesized following the synthetic pathway described for compound **8** in Scheme 1 of the main text (61 mg, 57%). ^{1}H NMR (600 MHz, DMSO-d_6) δ 3.51 (d, *J* = 5.9, 2H), 4.13 (d, *J* = 5.3, 2H), 4.62 (s, 2H), 6.78 (m, 2H), 6.87 (m, 1H), 7.17 (dd, *J* = 5.0, *J* = 3.7, 1H), 7.60 (dd, *J* = 3.7, *J* = 1.3, 1H), 7.93 (dd, *J* = 5.0, *J* = 1.3, 1H), 8.17 (t, *J* = 5.8, 1H), 8.37 (t, *J* = 5.9, 1H), 10.69 (s, 1H); ^{13}C NMR (150 MHz, DMSO) δ 41.7, 45.4, 66.8, 115.1, 115.9, 122.2, 127.0, 127.6, 131.8, 132.6, 133.3, 140.9, 142.2, 165.0, 167.2; HRMS (ESI): calcd for $C_{15}H_{16}N_3O_5S_2$ [M+H]$^+$ 382.0526, found 382.0537.

4-(5-(Methylsulfonyl)indolin-1-yl)-4-oxo-*N*-((3-oxo-3,4-dihydro-*2H*-benzo[1,4]oxazin-6-yl)methyl)butanamide (18). Compound **18** was synthesized following the synthetic pathway described for compound **8** in Scheme 1 of the main text (32 mg, 32%). ^{1}H NMR (600 MHz, DMSO-d_6) δ 2.48 (t, *J* = 7.0, 2H), 2.74 (t, *J* = 6.7, 2H), 3.50 (s, 3H), 3.33(t, *J* = 8.3, 2H), 4.16 (d, *J* = 6.0, 2H), 4.21 (t, *J* = 8.6, 2H), 4.52 (s, 2H), 6.79 (d, *J* = 1.9, 1H), 6.82 (dd, *J* = 5.0, *J* = 2.0, 1H), 6.87 (ds, *J* = 8.2, 1H), 7.72 (dd, *J* = 8.5, *J* = 2.0, 1H), 7.75 (ds, *J* = 1.3, 1H), 8.20 (d, *J* = 8.5, 1H), 8.39 (t, *J* = 6.0, 1H), 10.69 (s, 1H); ^{13}C NMR (150 MHz, DMSO) δ 27.0, 29.6, 30.6, 41.6, 43.9, 49.0, 66.8, 114.8, 115.3, 115.9, 122.0, 123.6, 127.1, 127.2, 133.2, 133.9, 134.7, 142.1, 147.2, 165.0, 171.0, 171.4; HRMS (ESI): calcd for $C_{22}H_{24}N_3O_6S$ [M+H]$^+$ 458.1380, found 458.1379.

5-Oxo-*N*-((3-oxo-3,4-dihydro-*2H*-benzo[1,4]oxazin-6-yl)methyl)pyrrolidine-2-carboxamide (19). Compound 1**9** was synthesized following the synthetic pathway described for compound **8** in Scheme 1 of the main text (19 mg, 56%). ^{1}H NMR (400 MHz, DMSO-d_6) δ 1.90 (m, 1H), 2.18 (m, 3H), 4.01 (dd, *J* = 8.1, *J* = 4.6, 1H), 4.17 (td, *J* = 14.8, *J* = 6.0, 2H), 4.53 (s, 2H), 6.78 (d, *J* = 2.0, 1H), 6.81 (dd, *J* = 8.1, *J* = 2.0, 1H), 6.88 (ds, *J* = 8.1, 1H), 7.80 (s, 1H), 8.46 (t, *J* = 5.9, 1H), 10.71 (s, 1H); ^{13}C NMR (100 MHz, DMSO) δ 25.4, 29.3, 41.5, 55.8, 66.8, 114.8, 115.9, 122.0, 127.1, 133.5, 142.2, 165.0, 172.3, 177.4; HRMS (ESI): calcd for $C_{14}H_{16}N_3O_4$ [M+H]$^+$ 290.1135, found 290.1147.

2,6-Dioxo-*N*-((3-oxo-3,4-dihydro-*2H*-benzo[1,4]oxazin-6-yl)methyl)-1,2,3,6-tetrahydropyrimidine-4-carboxamide (20). Compound **20** was synthesized following the synthetic pathway described for compound **8** in Scheme 1 of the main text (33 mg, 85%). ^{1}H NMR (600 MHz, DMSO-d_6) δ 4.30 (d, *J* = 5.9, 2H), 4.53 (s, 2H), 6.06 (s, 1H), 6.82 (d, *J* = 2.0, 1H), 6.85 (dd, *J* = 8.2, *J* = 2.0, 1H), 6.89 (ds, *J* = 8.2, 1H), 9.33 (t, *J* = 5.9, 1H), 10.69 (s, 1H), 10.72 (s, 1H), 11.27 (s, 1H); ^{13}C NMR (150 MHz, DMSO) δ 42.2, 66.8, 99.9, 114.8, 116.0, 122.2, 127.2, 132.5, 142.3, 145.0, 150.7, 160.0, 164.1, 164.9; HRMS (ESI): calcd for $C_{14}H_{13}N_4O_5$ [M+H]$^+$ 317.0880, found 317.0882.

4-(Indolin-1-yl)-4-oxo-*N*-((3-oxo-3,4-dihydro-*2H*-benzo[1,4]oxazin-6-yl)methyl)butanamide (21). Compound **21** was synthesized as described for compound **8** in Scheme 1 of the main text (51 mg, 61%). ^{1}H NMR (600 MHz, DMSO-d_6) δ 2.47 (t, *J* = 6.9, 2H), 2.69 (t, *J* = 6.8, 2H), 3.14 (t, *J* = 8.4, 2H), 4.11 (t, *J* = 8.6, 2H), 4.16 (d, *J* = 5.9, 2H), 4.52 (s, 2H), 6.82 (m, 3H), 6.97 (t, *J* = 7.4, 1H), 7.13 (t, *J* = 7.8, 1H), 7.22 (d, *J* = 7.4, 1H), 8.05 (d, *J* = 8.0, 1H), 8.36 (t, *J* = 5.9, 1H), 10.67 (s, 1H); ^{13}C NMR (100 MHz, DMSO) δ 27.3, 29.8, 30.4, 41.6, 47.2, 66.7, 114.8, 115.8 (2C), 121.9, 123.0, 124.7, 126.8, 127.0, 131.6, 133.8, 142.0, 142.9, 164.9, 170.1, 171.2; HRMS (ESI): calcd for $C_{21}H_{22}N_3O_4$ [M+H]$^+$ 380.1605, found 380.1606.

(*E*)-3-(4-Bromothiophen-2-yl)-*N*-((3-oxo-3,4-dihydro-*2H*-benzo[1,4]oxazin-6-yl)methyl)acrylamide (22). Compound **22** was synthesized as described for compound **8** in Scheme 1 of the main text (51 mg, 93%). ^{1}H NMR (400 MHz, DMSO-d_6) δ 4.28 (d, *J* = 5.9, 2H), 4.52 (s, 2H), 6.47 (d, *J* = 15.6, 1H), 6.82 (s, 1H), 6.86 (m, 2H), 7.43 (s, 1H), 7.56 (d, *J* = 15.6, 1H), 7.72 (s, 1H), 8.60 (t, *J* = 5.9, 1H), 10.67 (s, 1H); ^{13}C NMR (100 MHz, DMSO) δ 41.8, 66.7, 109.6, 114.8, 115.9, 122.0, 122.1, 125.0, 127.1, 130.8, 131.8, 133.4,

141.1, 142.2, 164.1, 164.8; HRMS (ESI): calcd for $C_{16}H_{14}BrN_2O_3S$ $[M+H]^+$ 292.9900, found 292.9903.

(*E*)-*N*-((3-oxo-3,4-dihydro-*2H*-benzo[1,4]oxazin-6-yl)methyl)-3-(4-(trifluoromethyl)phenyl)acrylamide (23). Compound **23** was synthesized as described for compound **8** in Scheme 1 of the main text (57 mg, 69%). ^{1}H NMR (600 MHz, DMSO-d_6) δ 4.32 (d, *J* = 5.3, 2H), 4.53 (s, 2H), 6.81 (dd, *J* = 15.8, *J* = 1.7, 1H), 6.85 (s, 1H), 6.88 (m, 2H), 7.54 (dd, *J* = 15.8, *J* = 1.5, 1H), 7.78 (m, 4H), 8.68 (t, *J* = 5.2, 1H), 10.69 (s, 1H); ^{13}C NMR (150 MHz, DMSO) δ 41.9, 66.8, 115.0, 116.0, 112.2, 124.1 (q, *J* = 270.5 Hz), 124.8, 125.8 (q, *J* = 3.8 Hz, 2C), 127.2, 128.1 (2C), 129.2 (q, *J* = 31.6 Hz), 133.5, 137.3, 139.0, 142.2, 164.4, 165.0; HRMS (ESI): calcd for $C_{19}H_{16}F_3N_2O_3$ $[M+H]^+$ 377.1108, found 377.1120.

(*E*)-3-(*1H*-Imidazol-4-yl)-*N*-((3-oxo-3,4-dihydro-*2H*-benzo[1,4]oxazin-6-yl)methyl)acrylamide (24). Compound **24** was synthesized as described for compound **8** in Scheme 1 of the main text (20 mg, 61%). ^{1}H NMR (400 MHz, DMSO-d_6) δ 4.26 (d, *J* = 6.0, 2H), 4.52 (s, 2H), 6.54 (d, *J* = 15.4, 1H), 6.85 (m, 3H), 7.34 (d, *J* = 15.4, 1H), 7.40 (s, 1H), 7.74 (s, 1H), 8.49 (t, *J* = 6.0, 1H), 10.68 (s, 1H), 12.28 (s, 1H); ^{13}C NMR (100 MHz, DMSO) δ 41.6, 66.8, 114.8, 115.9, 118.2, 121.1, 122.0, 127.1, 131.0, 134.0, 135.4, 137.1, 142.1, 165.0, 165.6; HRMS (ESI): calcd for $C_{15}H_{15}N_4O_3$ $[M+H]^+$ 299.1139, found 299.1138.

(*E*)-3-(5-Nitrofuran-2-yl)-*N*-((3-oxo-3,4-dihydro-*2H*-benzo[1,4]oxazin-6-yl)methyl)acrylamide (25). Compound **25** was synthesized as described for compound **8** in Scheme 1 of the main text (37 mg, 49%). ^{1}H NMR (600 MHz, DMSO-d_6) δ 4.30 (d, *J* = 6.0, 2H), 4.53 (s, 2H), 6.83 (m, 3H), 6.90 (d, *J* = 8.0, 1H), 7.15 (d, *J* = 3.8, 1H), 7.37 (d, *J* = 15.7, 1H), 7.75 (d, *J* = 3.8, 1H), 8.87 (t, *J* = 5.8, 1H), 10.69 (s, 1H); ^{13}C NMR (150 MHz, DMSO) δ 41.9, 66.8, 114.7, 114.8, 116.0, 116.1, 122.1, 124.8, 125.7, 127.2, 133.2, 142.2, 151.6, 153.3, 163.5, 165.0; HRMS (ESI): calcd for $C_{16}H_{14}N_3O_6$ $[M+H]^+$ 344.0877, found 344.0887.

(*E*)-4-(4-Chlorophenyl)-4-oxo-*N*-((3-oxo-3,4-dihydro-*2H*-benzo[1,4]oxazin-6-yl)methyl)but-2-enamide (26). Compound **26** was synthesized as described for compound **8** in Scheme 1 of the main text (41 mg, 50%). ^{1}H NMR (400 MHz, DMSO-d_6) δ 4.32 (d, *J* = 5.8, 2H), 4.53 (s, 2H), 6.87 (m, 3H), 7.03 (d, *J* = 15.3, 1H), 7.64 (d, *J* = 8.6, 2H), 7.79 (d, *J* = 15.4, 1H), 8.3 (d, *J* = 8.6, 2H), 9.06 (t, *J* = 6.0, 1H), 10.69 (s, 1H); ^{13}C NMR (100 MHz, DMSO) δ 42.0, 66.7, 115.0, 116.0, 122.2, 127.2, 129.1 (2C), 130.6 (2C), 131.9, 132.9, 135.2, 136.6, 138.7, 142.3, 163.2, 164.9, 188.8; HRMS (ESI): calcd for $C_{19}H_{16}ClN_2O_4$ $[M+H]^+$ 371.0793, found 371.0796.

UPLC-MS analysis. Analysis was performed using a Bruker-Q II TOF electrospray mass spectrometer coupled with Dionex UltiMate 3000 ultra high-pressure liquid chromatography instrument. A Thermo Scientific Acclaim TM RSLC 120 (C18, 2 µm, 120 Å, 2.1 x 100 mm) column was used at 40 °C. The mobile phases were supplemented with 0.1% formic acid and the following chromatographic conditions were used: 10% water/90% acetonitrile for 1 min, an 8-min linear gradient to 100% water, and to 10% water/90% acetonitrile at 8.1 min with a flow rate of 0.4 mL/min and UV/Vis detection at 240 nm.

Molecular dynamics. The coordinates of MMP-8, MMP-13 and MMP-14 (PDB IDs 2YO4, 456C, and 3MA2 respectively) were downloaded from the Protein Data Bank (rcsb.org). All three X-ray structures contained atomic coordinates for the loop region. For MMP-13, the coordinate selection was based on superimposition to the other two X-ray structures; all three structures showed nearly identical loop conformation upon structural superimposition (Figure 1D). The coordinates were prepared with the Maestro program (v9.7, Schrodinger LLC, NY, USA). During the process, bond orders were assigned and hydrogen atoms were added. The zinc-chelator inhibitor from PDB structure 456C was removed. Further, protonation states were assigned for the metal-coordinated histidine residues. Crystallographic positions of water molecules coordinated to the catalytic Zn^{2+} ions (PDB ID: 2YO4) were retained in the modeling. Molecular-dynamics simulations were performed with the AMBER14 suite.[2] Protein was solvated with a truncated octahedron box of TIP3P water model with box sides at least 10 Å away from the protein surface. The system was neutralized by the addition of either Cl^- or Na^+. Amberff12SB forcefield provided the necessary molecular-mechanics parameters. Energy minimization was performed for the water molecules for a maximum of 2000 steps and subsequently the entire system was energy minimized for another 2000 steps. The system was heated to 300 ºK and equilibration of the water molecules was performed for 400 ps. In the first equilibration stage of 400 ps, the protein side chains and water molecules were allowed to freely move while positional restraint with a force constant of 100 kcal/mol was applied to the backbone atoms (N, CA and C), Zn^{2+} ions and Ca^{2+} ions, as well as the residues coordinated with the ions. The restraints were reduced in the succeeding two equilibration stages of 400 ps. Production simulation for 500 ns was performed with CUDA GPU accelerated PMEMD module implemented in the AMBER14 suite.[3] Bonds to hydrogen atoms were constrained with SHAKE and 2 fs time step was used in the simulation. Berendsen barostat and thermostat were employed for pressure and temperature control, respectively. The distances of Zn^{2+} and Ca^{2+} atoms to the coordinated protein-residue atoms were restrained within 0.5 Å of the crystal structure distances by applying a parabolic well potential restraint of 20 kcal/(mol.Å). Post-simulation analysis was performed with cpptraj[4] module implemented in AMBER14 and VMD program.[5] Coordinates from the simulation were saved every 10 ps, resulting in a trajectory of 50,000 snapshots. The conformational snapshots from MMP-13 were grouped to 500 clusters based on the S1′ loop residue (Pro242-Pro255) backbone Cα atoms using cpptraj module of the AMBER14 program (hierarchical agglomerate approach algorithm with average-linkage). The representative snapshots from each cluster were visually inspected by the VMD program for the formation of space to accommodate substituted chemical groups in R1/R2 direction. From the 500 snapshots, we selected six MMP-13 conformations that allowed space for the desired substitution in the region and used them for the molecular docking calculation (described in the following section).

Focused library design. Electronic library of commercially available building blocks from vendor Sigma-Aldrich Corporation were obtained from the ZINC database. A virtual focused library with structural variations at R1 and R2 positions was generated by attaching the acid and ketone building blocks to the bezoxazinone core structure taking account of synthetic feasibility (Scheme 1). CombiGlide program (v. 3.2, Schrödinger, LLC, NY, USA) was utilized in the library design. Subsequently, the compounds were prepared using LigPrep program (v. 2.9, Schrödinger, LLC., NY, USA), in which protonation states within pH 7±2 was assigned and energy minimized using OPLS2005 forcefield.

Virtual screening of focused library by molecular docking. MMP-13 conformational snapshots were obtained from the

molecular-dynamics trajectory as explained above. Coordinates were subjected to energy minimization using Schrödinger Protein Preparation Wizard module. Molecular docking was performed using the Glide program (v 6.2; Schrödinger, LLC, NY, USA). Grid files were generated based on MMP-8 co-crystallized with compound **1** coordinate position (PDB ID: 3DNG) as center of a cubic box of 30-Å size. The lead compound **1** was docked to all the six snapshots and two of the MMP-13 conformations could reproduce X-ray binding pose of the inhibitor within 1 Å of root-mean-squared deviation as top scoring solution. The previously prepared focused library of 28,099 compounds was docked to these two MMP-13 conformations. In order to prioritize compounds with superior predicted drug-likeness, those which violated more than one criterion of Lipinski's rule of five[6] and Jorgensen's rule of three[7] were discarded. The docked solutions were analyzed using the Maestro program. Visual inspection of higher-ranked compounds was performed for evaluating their interactions within the pocket. A set of 19 compounds was finally selected, giving preference to synthetic availability and structural class. Compounds **8 - 12** formed the first series of compounds that retained the same hydrogen-bond pattern as compound **1** to the loop. Compounds **13-26** structurally diverged from the parent compound **1** (Figure S5).

Table S3. Docking score and ranks of selected compounds from the library of 28,099 compounds (ranked on two MMP-13 MD snapshot conformations).

	SNAPSHOT-1		SNAPSHOT-2	
COMPOUND	*Rank*[†]	*Score*[‡]	*Rank*[†]	*Score*[‡]
8	960	-9.653	1217	-7.936
9	853	-9.694	1884	-7.654
10	2122	-9.325	458	-8.314
11	5795	-8.406	1730	-7.720
12	6055	-8.133	6101	-6.482
13	237	-8.427	252	-7.770
14	703	-8.094	612	-7.511
15	470	-8.226	1159	-7.295
16	677	-8.107	5211	-6.576
17	1198	-7.905	3184	-6.848
18	567	-8.161	347	-7.673
19	789	-8.050	6114	-6.477
20	5651	-7.088	1953	-7.075
21	3793	-7.385	3353	-6.823
22	3473	-7.433	7822	-6.261
23	2796	-7.542	6521	-6.434
24	3744	-7.393	7461	-6.314
25	4875	-7.213	6906	-6.384
26	823	-8.038	4205	-6.704

[†]Virtual screening ranks of the compounds based on docking score. Compounds are ranked within the series (series 1: 8-12, and series 2: 13-26). [‡]Glide docking score (kcal/mol).

Enzyme-inhibition studies. Human recombinant active MMP-2 and MMP-7, and the catalytic domains of MMP-3 and MMP-14/MT1-MMP were purchased from EMD Chemicals, Inc. (San Diego, CA, USA); human recombinant catalytic domains of MMP-1, MMP-8, MMP-9, MMP-12 and MMP-13 were purchased from Enzo Life Sciences, Inc. (Farmingdale, NY, USA). Fluorogenic substrates MOCAc-Pro-Leu-Gly-Leu-A2pr(Dnp)-Ala-Arg-NH_2 (for MMP-2, MMP-7, MMP-9 and MMP-14) and MOCAc-Arg-Pro-Lys-Pro-Val-Glu-Nva-Trp-Arg-Lys(Dnp)-NH_2 (for MMP-3) were purchased from Peptides International (Louisville, KY, USA); Mca-KPLGL-Dpa-AR-NH_2 (for MMP-1, MMP-8, and MMP-13) was purchased from R&D Systems (Minneapolis, MN, USA). Inhibitor stock solutions (10 mM) were prepared fresh in DMSO before assays. We followed the same methodology for enzyme inhibition studies as reported before by Page-McCaw *et al*.[8] Enzyme-inhibition studies were carried out using a Cary Eclipse fluorescence spectrophotometer (Varian, Walnut Creek, CA, USA).

Pharmacokinetic studies. Animals. Mice (male CD-1, 6-7 weeks old, ~35 g body weight, specific pathogen free) were purchased from Charles River Laboratories, Inc. (Wilmington, MA, USA). All the procedures to maintain the mice were the same as reported previously[9] and they were approved by the Institutional Animal Care and Use Committee at the University of Notre Dame.

Animal dosing and sample collection. For iv administration, compound **8** was formulated as a solution in 25% DMSO, 60% propylene glycol, 5% Tween 80, and 10% PBS at a concentration of 0.35 mg/mL; for po administration, compound **8** was formulated as a solution of 40% DMSO, 50% propylene glycol, and 10% PBS at a concentration of 3.5 mg/mL. Mice were given a single 100-µL iv or po dose of **8** (n = 3 per time point). The sterilization of the dosing solutions and the procedure for collection of plasma samples were the same as reported by Gooyit *et al*.[9]

Sample analysis. The preparation for both plasma samples and calibration curves for quantification purposes were the same as reported by Gooyit *et al*.[9] Samples were analyzed by ultraperformance liquid chromatography (UPLC)/(+)electrospray ionization (ESI)-multiple-reaction monitoring (MRM) with a reversed-phase C18 column (Kinetex 1.7u C18 100A, 100 × 2.10 mm, Phenomenex, Torrance, CA, USA), coupled with a SecurityGuard ULTRA Cartridges (UHPLC C18 for 2.1 mm ID columns, Phenomenex, Torrance, CA, USA). We used compound **1** as internal standard. The MRM transitions were 501→162 for compound **8** and 461→162 for compound **1**. Quantification method was the same as reported.[9] The mass spectrometric acquisition for both **1** and **8** were performed in the positive ESI mode with MRM methods. The capillary voltage, cone voltage, extractor voltage, and RF lens voltage were 3 kV, 45 V, 3 V, and 0.1 V, respectively. Desolvation and cone gas (nitrogen) flow rates were 550 L/h and 40 L/h, respectively. The source and desolvation temperature were held at 100 and 150 °C, respectively. The elution method for mobile phase were: flow rate at 0.5 mL/min, 70% water/30% acetonitrile for 1 min, followed by a 5-min linear gradient to 5% water/95% acetonitrile and kept for 2 min, followed by a 1-min linear gradient back to 70% water/30% acetonitrile and kept for the final 1 min.

Pharmacokinetic parameters. The area under the mean concentration-time curve (*AUC*), *CL*, *Vd*, and $t_{1/2}$ were obtained from the report generated by Phoenix WinNonlin software version 6.3 (Certara USA, Inc, Princeton, NJ, USA). The bioavailability was calculated by the formula: $F = AUC_{po} \cdot D_{iv} / AUC_{iv} \cdot D_{po} \times 100\%$, where F is the absolute oral bioavailability; AUC_{po} and AUC_{iv} are the *AUC* for po and iv administrations, respectively; D_{po} and D_{iv} are the doses for po and iv administrations, respectively.

Supporting information movie. The movie shows dynamic motion of the Phe252 residue in MMP-13 during the 500 ns simulation. Due to the high flexibility of the loop, the residue experienced significant displacement. In order to show the most relevant motion, movie is played in different speed rate than the actual time scale.

References:

(1) Ding, D. R.; Lichtenwalter, K.; Pi, H. L.; Mobashery, S.; Chang, M. Characterization of a selective inhibitor for matrix metalloproteinase-8 (MMP-8). *Medchemcomm.* **2014,** 5, 1381-1383.

(2) Case, D. A.; Babin, V.; Berryman, J. T.; Betz, R. M.; Cai, Q.; Cerutti, D. S.; Cheatham, T. E.; Darden, T. A.; Duke, R. E.; Gohlke, H.; Goetz, A. W.; Gusarov, S.; Homeyer, N.; Janowski, P.; Kaus, J.; Kolossváry, I.; Kovalenko, A.; Lee, T. S.; LeGrand, S.; Luchko, T.; Luo, R.; Madej, B.; Merz, K. M.; Paesani, F.; Roe, D. R.; Roitberg, A.; Sagui, C.; Salomon-Ferrer, R.; Seabra, G.; Simmerling, C. L.; Smith, W.; Swails, J.; Walker; Wang, J.; Wolf, R. M.; Wu, X.; Kollman, P. A. *AMBER 2014*. University of California, San Francisco, 2014.

(3) Gotz, A. W.; Williamson, M. J.; Xu, D.; Poole, D.; Le Grand, S.; Walker, R. C. Routine Microsecond Molecular Dynamics Simulations with AMBER on GPUs. 1. Generalized Born. *J. Chem. Theory Comput.* **2012,** 8, 1542-1555.

(4) Roe, D. R.; Cheatham, T. E., 3rd. PTRAJ and CPPTRAJ: Software for Processing and Analysis of Molecular Dynamics Trajectory Data. *J. Chem. Theory Comput.* **2013,** 9, 3084-95.

(5) Humphrey, W.; Dalke, A.; Schulten, K. VMD: visual molecular dynamics. *J. Mol. Graph.* **1996,** 14, 33-8, 27-8.

(6) Lipinski, C. A.; Lombardo, F.; Dominy, B. W.; Feeney, P. J. Experimental and computational approaches to estimate solubility and permeability in drug discovery and development settings. *Adv. Drug. Deliv. Rev.* **2001,** 46, 3-26.

(7) Jorgensen, W. L.; Duffy, E. M. Prediction of drug solubility from structure. *Adv. Drug. Deliv. Rev.* **2002,** 54, 355-66.

(8) Page-McCaw, A.; Ewald, A. J.; Werb, Z. Matrix metalloproteinases and the regulation of tissue remodelling. *Nat. Rev. Mol. Cell Biol.* **2007,** 8, 221-33.

(9) Gooyit, M.; Song, W.; Mahasenan, K. V.; Lichtenwalter, K.; Suckow, M. A.; Schroeder, V. A.; Wolter, W. R.; Mobashery, S.; Chang, M. O-phenyl carbamate and phenyl urea thiiranes as selective matrix metalloproteinase-2 inhibitors that cross the blood-brain barrier. *J. Med. Chem.* **2013,** 56, 8139-50.